

Available online at [www.sciencedirect.com](http://www.sciencedirect.com)

Surface &amp; Coatings Technology 188–189 (2004) 745–749

[www.elsevier.com/locate/surfcoat](http://www.elsevier.com/locate/surfcoat)

# Biocompatibility of a titanium–aluminum nitride film coating on a dental alloy

K.H. Chung<sup>a,\*</sup>, G.T. Liu<sup>b</sup>, J.G. Duh<sup>b</sup>, J.H. Wang<sup>c</sup><sup>a</sup>*Institute of Oral Biology, School of Dentistry, National Yang-Ming University, Taipei 112, and Dental Department, Kaohsiung Veterans General Hospital, Kaohsiung 813, Taiwan*<sup>b</sup>*Department of Material Science and Engineering, National Tsing-Hua University, Hsinchu 300, Taiwan*<sup>c</sup>*Chunghwa Telecom Co. Ltd, Yang-Mei, Taoyuan, Taiwan*

Available online 26 August 2004

## Abstract

The purpose of this investigation was to develop a coating technique and to study the characteristics of titanium–aluminum nitride [(Ti,Al)N] films deposited on a base-metal alloy (Wiron88<sup>®</sup>) substrate. Titanium–aluminum nitride thin films were deposited on the alloy surface using a reactive radiofrequency sputtering method. The electrochemical properties of three specimens with and without coating treatment were evaluated. The biocompatibility of the three specimens was tested using a subcutaneous implantation test. Data were analyzed using the *t*-test with a significance level of  $p < 0.05$ . Specimens coated with (Ti,Al)N films exhibited significantly improved corrosion resistance ( $p < 0.05$ ). The results from biocompatibility testing, based on tissue reactions at 2 and 12 weeks, revealed substantially enhanced biocompatibility for (Ti,Al)N-coated samples when compared to uncoated samples. This demonstrates that the (Ti,Al)N film can significantly improve electrochemical and biocompatibility properties of the base metal alloy.

© 2004 Elsevier B.V. All rights reserved.

**Keywords:** Titanium–aluminum nitride film coating; Base-metal alloy; Electrochemical property; Biocompatibility

## 1. Introduction

Nickel-based alloys have historically exhibited an acceptable combination of strength, hardness and porcelain compatibility for metal-ceramic restorations [1]. Nevertheless, the release of nickel has been reported owing to the multiple phases of the nickel-based alloys [2–4]. Concern exists regarding the biocompatibility of the nickel-based alloys used intraorally, especially for patients with known nickel sensitivity [5]. The incidence of adverse reaction to nickel has been reported to be 5–10 times higher for females than for males, with 5% to 8% of females showing sensitivity [6–10]. However, local and systemic responses to nickel-based alloys secondary to intraoral corrosion and dissolution have not been adequately investigated [11]. In

order to improve the biocompatibility and surface characteristics of base-metal alloys for dental appliance fabrication, the physical masking of the alloy surface using biocompatible barriers, or coatings, has been attracted considerable attention [12]. The procedure involves using an intermediate layer deposited on the alloy surface after the construction of dental appliance. The deposited layer should be biocompatible and serves as a barrier to the diffusion of adverse components. It must also be strongly adherent to the metal substrate.

Favorable biocompatibility, electrochemical properties, and mechanical properties are essential to the widespread acceptance of newly developed materials for biomedical applications. Universal agreement is not available regarding the most appropriate method for biocompatibility testing. The International Standard Organization (ISO) has attempted to correlate a description of the tissue reaction to materials in order to define adequate biological acceptance [13]. Akagawa et al. [14] and Wolfaardt et al. [15] used a subcutaneous

\* Corresponding author.

*E-mail addresses:* chungkh@ym.edu.tw, chungk@uthscsa.edu (K.H. Chung).

implantation test to assess ceramic and impression materials, respectively, based on the ISO Technical Report 7405 [13]. Parameters, such as capsule thickness and inflammatory response, were used to determine biocompatibility. In fact, biocompatibility with metal corrosion products is of fundamental importance. The release of elements from corroding alloys may lead to adverse biologic effects, such as toxicity, allergy, or mutagenicity [9].

Recent studies have focused on titanium nitride, designated TiN, film deposition to serve as a diffusion barrier in microelectronic circuitry and clinical dentistry [12,16–18]. Due to excellent hardness and wear resistance, the TiN film coating has also been considered for use in orthopedic prostheses and cardiac valves [19–21]. In the construction of metal-ceramic crowns, several layers of dental porcelain are typically fused onto the external surface of a metal substructure in order to mask the metallic color and produce natural tooth-like dental restoration [1]. Investigations addressing bond characteristics between dental porcelain and TiN-film-coated dental alloys have demonstrated a deterioration of adhesion between the TiN film and substrate alloys during porcelain firing. In fact, the evaporation point of the TiN film was estimated to be 550 °C. The (Ti,Al)N film demonstrates even more stable pyrochemical properties and an evaporation point higher than 800 °C [22,23]. It is argued that a (Ti,Al)N film can be used as an intervening layer to improve the biocompatibility of metal substrate in dental application. The purpose of this investigation was to develop a (Ti,Al)N film coating technique and to study the surface characteristics of this (Ti,Al)N film on a dental base-metal alloy substrate.

## 2. Experimental details

### 2.1. Metal substrate preparation

Inlay casting wax (Blue inlay casting wax, Type II, Kerr Mfg. Romulus, MI) patterns were fabricated from silicone molds with recess dimensions of 15×15×1.5 mm (plate) and 3×10×1.5 mm (strip), respectively. Wax patterns were sprued and invested in a phosphate-bonded material (Fujinvest, GC, Tokyo, Japan). A nickel-based dental alloy was used to complete the castings: Wiron88® (Lot no. 9544, Bego, Postfach, Germany) containing mainly 64% Ni, 24% Cr, and 10% Mo. All manufacturer recommendations for wax elimination and metal casting were followed. The completed castings were divested and the sprues removed. Any remaining investment material was carefully removed using air abrasion with 110- $\mu$ m aluminum oxide. All castings were then ultrasonically cleaned for 15 min in distilled water. The resulting metal plates were randomly divided into two groups containing five specimens each. Six strip castings were constructed and used for the biocompatibility test. The metal surface was finished and polished metallurgically with silicone

carbide sandpapers (Buehler, Lake Bluff, IL) to 1200 grip. The ground surfaces were then polished with 1.0- $\mu$ m aluminum powder (MICROPOLISH 1.0 micro alpha alumina, Buehler) slurry in order to obtain a uniform surface condition for film coating and using as controls. Following surface finishing and polishing, specimens were ultrasonically cleaned in a solution of 99.8% methanol and distilled water for 15 min to remove any residue or debris.

### 2.2. Deposition of titanium–aluminum nitride film

Titanium–aluminum nitride films were deposited on the superior surface of metal plate and strip samples using a reactive radiofrequency sputtering procedure [23,24]. The sputtered coatings were deposited in a multigun sputtering deposition system with Ti and Al targets and reactive nitrogen gas as the sputtering sources. A schematic diagram of the deposition apparatus is shown in Fig. 1. After loading of the substrate and targets, the vacuum chamber was degassed down to  $2.7\times 10^{-3}$  Pa followed by the inlet of argon and nitrogen gases as plasma source and reactive gas, respectively, to a working pressure of 0.4 Pa. The target-to-substrate distance was kept at 60 mm from both sputtering target sources. Before deposition, both Ti and Al targets were presputtered for 5 min in order to clean the target surfaces. During sputtering, the radiofrequency powers for the Ti and Al target were fixed at 200 W. Initially, each metal plate or strip specimen was positioned in the target stage, facing the Ti and Al targets, and preheated to 350 °C for up to an hour. Argon gas was introduced into the chamber and presputtering with (Ti,Al) metallic film was performed on the specimen for 5 min. This (Ti,Al) film served as an interlayer between the metal substrate and nitride implantation. Next nitrogen gas filled the chamber along with the argon gas for the final sputtering processing. Argon (Ar) to nitrogen (N<sub>2</sub>) gas flow ratio of 1:3 was maintained by a mass flow controller (FC-280/FM-380 flow controller, Tylan, Stanford, CA). The (Ti,Al)N film sputtering was accomplished at a working pressure of  $4.0\times 10^{-1}$  Pa for 2 h. Through interaction between the vaporized titanium and aluminum metals and the reactive nitrogen gas, a nitridation of the (Ti,Al) metallic films was achieved by implantation of nitrogen ions. After nitrogen implantation in (Ti,Al) metallic film, a (Ti,Al)N solid solution was formed in the implanted layer [22]. Upon completion of (Ti,Al)N film deposition, the working chamber was vented and cooled to room temperature ( $25\pm 1$  °C).

### 2.3. Electrochemical testing

The corrosion and electrochemical behavior of five uncoated and (Ti,Al)N-film-coated samples were studied in Ringer's solution: 9.00g/l NaCl, 0.20g/l NaHCO<sub>3</sub>,

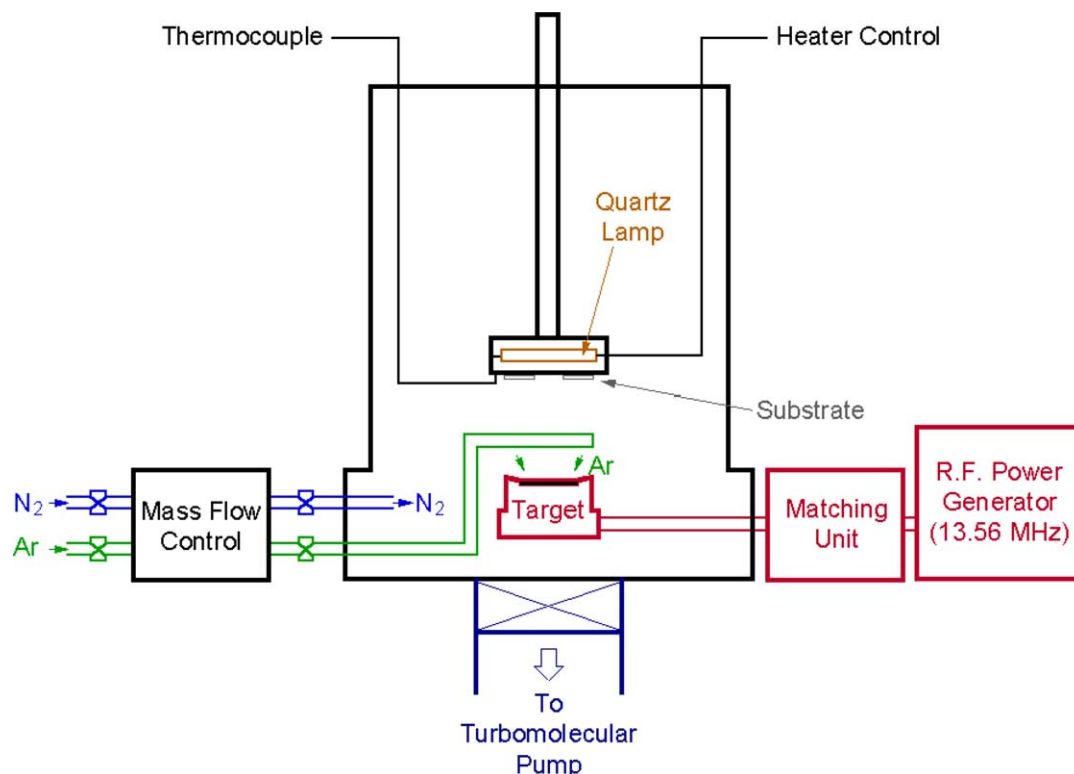


Fig. 1. Schematic diagram of the deposition apparatus.

0.25g/l  $\text{CaCl}_2 \cdot 6\text{H}_2\text{O}$ , 0.40g/l KCl [25]. The solution was prepared with analytically pure reagents and doubly distilled water. Uncoated alloy substrates and (Ti,Al)N-film-coated specimens were masked with silicone rubber to define the tested surface approximately  $10 \times 10$  mm. Specimen was employed as working electrode. A saturated Ag/AgCl reference electrode was used and a platinum plate served as the counter electrode. For electrochemical testing, the open-circuit potential (OCP) of each specimen was monitored for 24 h after immersion in Ringer's solution in order to attain steady-state conditions [25]. A linear polarization test was then performed with a potentiostat (Model 273, EG and G Instruments, Princeton Applied Research, Princeton, NJ). Each specimen was polarized from  $-50$  mV referred to the OCP. The potentiostat with computer-aided control provided a voltage range approximately from  $-1500$  to  $+2500$  mV at a scanning rate of  $1$  mV/s. The polarization curve was then recorded and analyzed.

#### 2.4. Biocompatibility testing

In order to evaluate tissue compatibility and biocompatible of the (Ti,Al)N film, tissue reaction assessment was conducted through 12 weeks of subcutaneous implantation in guinea pigs. Six guinea pigs were used, fully anesthetized with ethyl ether, and subjected to standard surgical techniques. The dorsal midline region of the animal was shaved. Two, 1-in. incisions were made

through the skin to the right and left of the midline. Starting from the incision, a pocket was prepared with blunt dissection into the subcutaneous tissue of each dorsal quadrant. Six strip specimens with (Ti,Al)N-film-coated top surfaces and uncoated bottom surfaces were autoclave sterilized for 20 min. A metal specimen was implanted in each of the right subcutaneous pockets. A  $10 \times 1.5$  mm polytetrafluoroethylene (PTFE) membrane (Lot No. D362M, GORE-TEX Regenerative Material, W.L. Gore and Associates, Flagstaff, AZ) was implanted in each of the left pockets as controls. Incisions were sutured. All animals were maintained on a standard laboratory diet and water.

At weeks 2 and 12 postoperation, three guinea pigs were sacrificed, respectively. Tissue blocks containing the tested specimen were excised and fixed in 10% neutral-buffered formalin. The metal strips were carefully removed from the tissue blocks after fixation and tissue specimens were embedded in paraffin according to routine histologic procedure. Sections with  $6 \mu\text{m}$  in thickness were prepared and stained with hematoxylin–eosin (H and E) stain. The sections were examined by light microscopy at magnification of  $250\times$  to determine the tissue reaction after short-term embedment.

#### 2.5. Statistical analysis

Polarization curve data and the thicknesses of the fibrous capsule were statistically analyzed with a *t*-test.

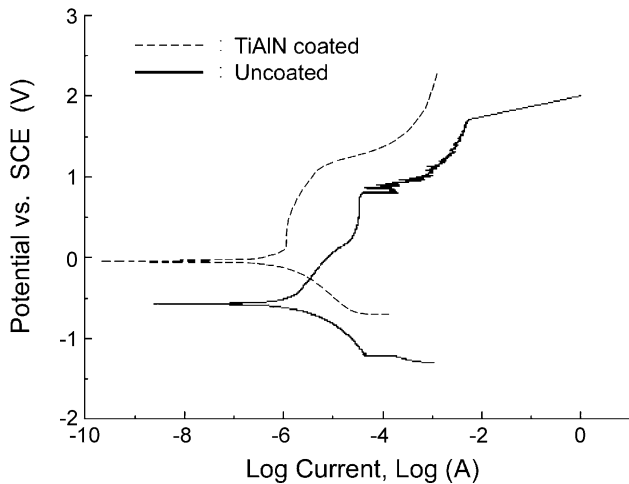


Fig. 2. Representative polarization curves of uncoated and (Ti,Al)N-film-coated Wiron88<sup>®</sup> specimens in Ringer's solution.

The critical level of statistical significance was chosen to be  $p < 0.05$ .

### 3. Results

The representative polarization curves of each group in Ringer's solution obtained at the potential sweep of 1 mV/s are presented in Fig. 2. The corrosion current density ( $I_{\text{corr}}$ ), corrosion potential ( $E_{\text{corr}}$ ), and resistance ( $R_p$ ) were calculated from polarization curves by fitting the Tafel equation, Table 1. The corrosion current density of the coated alloy substrate decreased significantly from approximately 835 to 368 nA/cm<sup>2</sup> ( $p < 0.05$ ). Throughout all immersion periods, the corrosion potentials of the (Ti,Al)N-film-coated sample (−79 mV) were much more positive than that of untreated base-metal alloy sample (−675 mV). The corrosion resistance of coated sample increased significantly to 68 from 13 kΩ of the untreated base-metal alloy sample.

Results of biocompatibility testing demonstrated fibrous encapsulation with local infiltration around both tested and control materials at 2 weeks. Inflammatory response was minimal inside the fibrous capsule around the surface of coated substrate. At the 12-week period, all tested materials were completely encapsulated by mature fibrous connective tissue and showed no evidence of active proliferation, as indicated in Fig. 3. However, increased

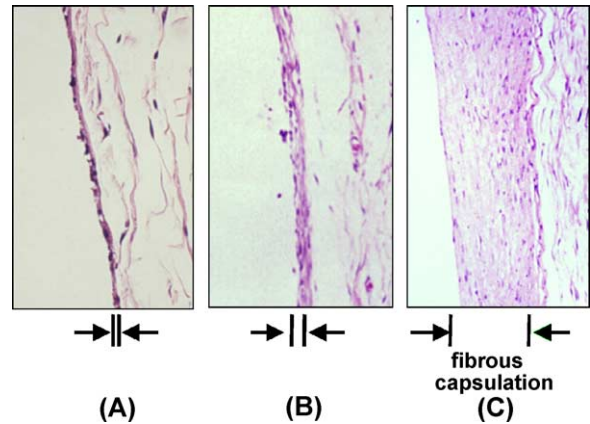


Fig. 3. Representative histologic pictures of fibrous connective tissue encapsulation around tested materials at 12 weeks. (A) Polytetrafluoroethylene membrane, (B) titanium–aluminum nitride film coating surface, and (C) uncoated nickel-based alloy surface. (H and E stain, original magnification 250×).

capsular thickness was revealed around the uncoated alloy surfaces.

### 4. Discussion

The chemical composition of the as-deposited (Ti,Al)N coating was measured by electron probe microanalyzer, combined with the ZAF correction method [26] using pure TiN as the reference standard material. Owing to the overlapping of the L spectra of titanium element with K spectra of nitrogen element, the spectrum deconvolution approach was adopted in order to acquire the composition of (Ti,Al)N precisely [23]. By varying the power on the Al target, the stoichiometric value of  $x$  in the  $\text{Ti}_{1-x}\text{Al}_x\text{N}$  coatings can be controlled accordingly. For aesthetic consideration in the dental application, the  $\text{Ti}_{0.75}\text{Al}_{0.25}\text{N}$  coating was selected in this study since the color of the  $\text{Ti}_{0.75}\text{Al}_{0.25}\text{N}$  film is similar to the oral mucosa with light purple in color.

Passivity in body fluids is a major consideration when working with base metal alloys for dental applications [25]. Stability of the passive condition of (Ti,Al)N-film-coated and uncoated nickel-based alloy can be revealed during the immersion period in the measurement of OCP. Uncoated nickel-based alloy is passive in a wider potential region up to the breakdown potential occurred at around +780 to +850 mV range. This can be seen in the anodic polarization curve (Fig. 2). Numerous spikes of anodic current are observed in the region of passivity close to the breakdown potential in the polarization curve of uncoated controls. It is indicated that initiation and repassivation of metastable pits happen on the alloy surface during anodic polarization [25]. At potentials above the breakdown potential, anodic current gradually increases because of nucleation of oxidation products inside pits and development of a stable pitting environment. However, nickel-

Table 1  
Results of linear polarization test

Material	Uncoated surface	TiAlN-coated surface
$I_{\text{corr}}$ (nA/cm <sup>2</sup> )	835	368
$E_{\text{corr}}$ (mV)	−675	−79
Resistance (kΩ)	13	68

based alloy specimens coated with (Ti,Al)N film were passive within the tested potential range below +1200 mV. The results of electrochemical testing clearly illustrate the favorable effect of the reactive (Ti,Al)N film coating procedure on the corrosion resistance of nickel-based alloy. Apparently, a thin layer of (Ti,Al)N film is sufficient to protect nickel-based alloy surface effectively from localized corrosion attack. According to a previous study using electron microprobe analysis to evaluate a reactive radiofrequency sputtered (Ti,Al)N film, the coating thickness was estimated to be 2  $\mu\text{m}$  [22,23]. In this investigation, the thickness of the (Ti,Al)N film was also measured to be approximately 2  $\mu\text{m}$ . In addition, very low current is measured in the region of passivity during potentiostatic test for (Ti,Al)N-film-coated specimen. This current is approximately 10–15 times smaller than that of the uncoated alloy. Lower passive dissolution rate of the composition of nickel-based alloy with (Ti,Al)N film coating can be compared to its original alloy surface. The results of the short-term biocompatibility testing support the decrease of passive dissolution rates of nickel-based alloy after (Ti,Al)N film coating. Histologic findings in the biocompatibility test revealed that the (Ti,Al)N-film-coated alloy surface, which is the empty space at the right side of the microscopic picture in Fig. 3, was well tolerated in the subcutaneous tissue. Thin fibrous connective tissue encapsulation was observed around (Ti,Al)N-film-coated alloy surface and control groups at the short-term subcutaneous test, as shown in Fig. 3. However, dense and thick encapsulation around the uncoated surface was revealed. This indicates that biocompatibility of the (Ti,Al)N-film-coated nickel alloy surface compares favorably with that of PTFE control surface which is reported to be tissue compatible [13].

Because of the excellent biocompatibility, desirable electrochemical properties, and relatively low cost of (Ti,Al)N film deposition, its application is proved beneficial in dental apparatus construction in this study. Application of (Ti,Al)N film coating onto the surface of implant fixtures needs further investigation.

## 5. Conclusions

- (1) Titanium–aluminum nitride film, or (Ti,Al)N film, was successfully deposited on dental alloys by reactive radiofrequency sputtering method.
- (2) The (Ti,Al)N coating treatment was found to considerably improve the corrosion behavior of nickel-base alloy by lowering the anodic current in the passive region and increase the corrosion potential positively.
- (3) Histologic findings of a short-term subcutaneous implantation test supported the biocompatibility of the (Ti,Al)N-film-coated nickel alloy surface, which compared favorably to PTFE control surfaces.

## Acknowledgements

This work was partially supported by the National Science Council and Veterans General Hospital-Taipei and National Tsing-Hua University, Taiwan, Republic of China, Grants Nos. NSC87-2314-B-010-031, NSC92-2314-B-010-034, and VGHTH-87-06-1. This investigation was also partially supported by the Center for Nano-Science and Technology of the University System of Taiwan, Taiwan under Project No. 91B0502J4.

## References

- [1] J.W. McLean, 2nd ed., *The Science and Art of Dental Porcelain*, vol. II, Quintessence, Chicago, IL, 1982, p. 245.
- [2] D. Brune, *Biomaterials* 7 (1986) 163.
- [3] F.J. Gil, L.A. Sanchez, A. Espias, *Int. Dent. J.* 49 (1999) 361.
- [4] J.C. Wataha, S.K. Nelson, P.E. Lockwood, *Dent. Mater.* 17 (2001) 409.
- [5] K.J. Anusavice, *Phillips' Science of Dental Materials*, 10th ed., Saunders, Philadelphia, PA, 1996, p. 442.
- [6] J.P. Moffa, A.D. Guckes, M.A. Okawa, *J. Prosthet. Dent.* 30 (1973) 432.
- [7] C. Liden, *Sci. Total Environ.* 148 (1994) 283.
- [8] R.G. Craig, *Restorative Dental Materials*, 10th ed., Mosby, St. Louis, MO, 1997, p. 414.
- [9] J.C. Wataha, *J. Prosthet. Dent.* 83 (2000) 223.
- [10] N.J. Grimaudo, *Gen. Dent.* (2001) 498.
- [11] K.F. Leinfelder, *J. Am. Dent. Assoc.* 128 (1997) 37.
- [12] P.R. Mezger, N.H.J. Creugers, *J. Dent.* 20 (1992) 342.
- [13] Federation Dentaire Internationale-International Organization for Standardization, *Biological evaluation of dental materials—subcutaneous implant tests*. Technical Report 7405. London (1984), 35.
- [14] Y. Akagawa, M. Hashimoto, N. Kondo, *J. Prosthet. Dent.* 53 (1985) 681.
- [15] J.F. Wolfaardt, P. Cleaton-Johes, J. Lownie, G. Ackermann, *J. Prosthet. Dent.* 68 (1992) 331.
- [16] M.A. Nicolet, *Thin Solid Films* 52 (1978) 415.
- [17] M. Wittmer, *J. Vac. Sci. Technol.* A3 (1985) 1797.
- [18] A. Paschoal, E.C. Vanancio, L. Canale, L. Silva, D. Huerta-Vilca, A. Motheo, *Artif. Organs* 27 (2003) 461.
- [19] I. Dion, F. Rouais, L. Trut, *Biomaterials* 14 (1993) 169.
- [20] M.J. Pappas, G. Markis, F.F. Buechel, *Clin. Orthop.* 317 (1995) 64.
- [21] M.T. Raimondi, R. Pietrabissa, *Biomaterials* 21 (2000) 907.
- [22] C.T. Huang, J.G. Duh, *Surf. Coat. Technol.* 81 (1996) 164.
- [23] C.T. Huang, J.G. Duh, *Surf. Coat. Technol.* 71 (1995) 258.
- [24] K.H. Chung, J.G. Duh, D. Shin, D.R. Cagna, R.J. Cronin, *J. Biomed. Mater. Res. (Appl. Biomater.)* 63 (2002) 516.
- [25] D. Starosvetsky, I. Gotman, *Biomaterials* 22 (2001) 1853.
- [26] J.I. Goldstein, *Scanning Electron Microscopy and X-ray Microanalysis*, 2nd ed., Plenum Press, New York, 1992, p. 48.